Supplementary Information

Enhancing light emission of ZnO microwire-based diodes by piezo-phototronic effect

Qing Yang [1,2], Wenhui Wang[1], Sheng Xu[1] and Zhong Lin Wang[1,*]

[1] School of Material Science and Engineering, Georgia Institute of Technology, Atlanta, Georgia 30332-0245 USA

[2] State Key Laboratory of Modern Optical Instrumentation, Department of Optical Engineering, Zhejiang University, Hangzhou 310027, China

[*]To whom the correspondence should be addressed. Email: zhong.wang@mse.gatech.edu

Contents:

A. Fabrication methods and measurement system

A1. Device fabrication and experimental setup.

A single ZnO micro-/nanowire LED was fabricated by manipulating a wire on a trenched substrate. The Mg acceptor doping concentration was about $5\times10^{17}/cm^3$. The ZnO micro/nanowires were synthesized by a high-temperature thermal evaporation process[1]. Before fabricating a n-ZnO wire/p-GaN film LED, a 20-nm layer of Ni and 50-nm layer of Au were deposited by thermal evaporation on the p-GaN as the anode electrode; and a 100-nm layer of ITO was sputtered on the sapphire substrate as the cathode electrode, both followed by rapid thermal annealing in air at 500 ^oC for 5 min. Then, the GaN covered sapphire substrate was attached closely to an ITO coated sapphire substrate (a small trench was formed between the two substrates). A single ZnO micro-/nanowire was picked up from the glass substrate and transferred to the trenched substrates across the gap by micromanipulation (as shown in Fig. 1b inset and Fig. S2). A transparent PS film with thickness of 500 μm and width less than the length of ZnO wire was used to cover the NW, and an external stress was applied onto the PS film by an alumina rod connected to a piezo nanopositioning stage that was fixed on a 3D micromanipulation stage. The entire device was packaged using narrow transparent adhesive tapes to obtain a tight contacting between ZnO wire and GaN substrate (Fig. 1b inset).

The measurement system is built based on an inverted microscope and 3D micromanipulation stages (Fig. S1). A normal force was applied on the PS film by an alumina rod connected to a piezo nanopositioning stage with closed loop resolution 0.2 nm (Fig. S1). To calculate the strain on the wire, we need to know the stress added on the PS tape. The recorded deformation on the piezo nanopositioning stage is determined by the deformation of PS film and Kapton film, considering the dimension (Fig. S2) and Young's modulus of each element in the device.

In the experiment, we measured the output light intensity by spectrometer or CCD, which characterizes the optical power in a relative manner. We mainly focus on the relative change of the output light intensity as well as the quantum efficiency under different strain. We derive the change of quantum efficiency by analyzing the output light intensity and current under the applied strain. The data for investigating the influence of strain on light intensity and spectrum are recorded using a fiber optical

spectrometer. The integration of peak spectrum is considered as the relative emission light intensity. The data for studying the strain effect on the polarization are recorded using a CCD. The relative light output intensity is extracted by analyzing the brightness of the image.

In order to investigate the polarization of the electroluminescence, a linear polarizer was placed in front of the CCD and spectrometer. The polarization angle was varied by rotating the polarizer anticlockwise in reference to the ZnO wire, with 0^{o} corresponding to the polarizer parallel to the length of the ZnO wire (from ITO to GaN).

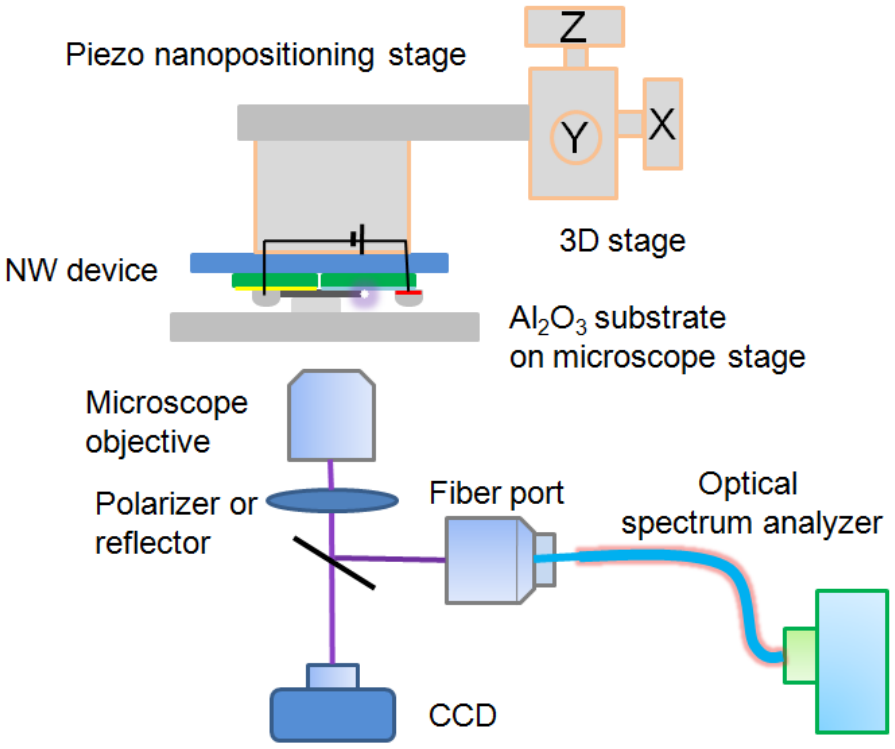

Fig. S1. Schematic diagram of the measurement system for characterizing the performance of a ZnO wire LED under applied compressive strain.

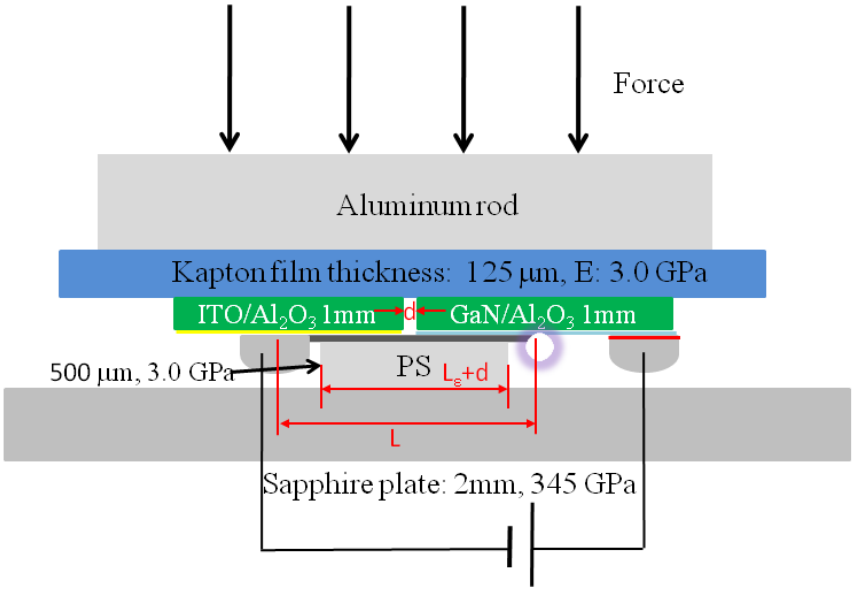

Fig. S2. Detailed side view of the device structure. GaN covered sapphire substrate is attached closely to an ITO coated sapphire substrate on a Kapton film. A single ZnO micro-/nanowire is placed across the two substrates. A transparent PS film with thickness of 500 μm is used to cover the wire and force is added on the PS film by an alumina rod connecting to a piezo nanopositioning stage (closed loop resolution 0.2 nm) fixed on a 3D micromanipulation stage. To calculate the strain on the wire, we need to know the stress added on the PS tape. Considering the dimension and Young's modulus of each element in the device, The recorded deformation on the piezo nanopositioning stage is determined by the deformation of PS film and Kapton film. Since the Young's modulus values of the Kapton film and PS film are both about 3 GPa, the thickness of the deformed film could be calculated as t=(500+125)=625 μm. If the recorded deformation of the film is δt and if the stress is uniform within the films in the contact area, the stress applied on PS film is (δt/t)×3 (GPa). The Young's modulus of ZnO is about 129 GPa. The strain in the ZnO wire can be calculated by (δt/t)×(3/129) ×100%=2.3δt/t%.

A2. Measurement of the external efficiency

We also measured the actual external efficiency of the single wire LED to quantify the absolute improvement in efficiency. Since the output of a single wire LED is low in total power so that we have taken a special design to measure the emission efficiency. We used the spectrometer to calibrate the power meter first. A 633 nm wavelength laser was input into the power meter and spectrometer simultaneously. Figure S3 shows the integrated intensity of the spectra as a function of the power read by the power meter. It can be seen that there is a linear relationship between them. Then we used the spectrometer to measure

the light intensity of the single NW LED. The emission power is estimated from the linear relationship in Fig. S3 by assuming the quantum efficiency of the spectrometer is the same for lights in the entire detection wavelength range.

In the experiment for measuring the external efficiency of a single wire LED, the output light is coupled by a pure silica fiber with diameter of 100 μm and guided into the spectrometer (Fig. S4a). We then calculated the optical power received by the spectrometer by analyzing the integrated intensity. In order to get the actual output power of the single wire LED, we also need to know the coupling efficiency between the silica fiber and the ZnO wire. We simulated the propagation and coupling behavior of the single wire LED by using a software program (BPM RSOFT) based on the beam-propagation method (Figs. S4b and S4c). The coupling efficiency of the structure we used in the experiment is about 34%. The external quantum efficiency was calculated by acquiring the ratio of the output light power and the input electrical power. Table 1 shows the room temperature external quantum efficiency versus voltage characteristics for the nanowire/thin film heterostructural LED.

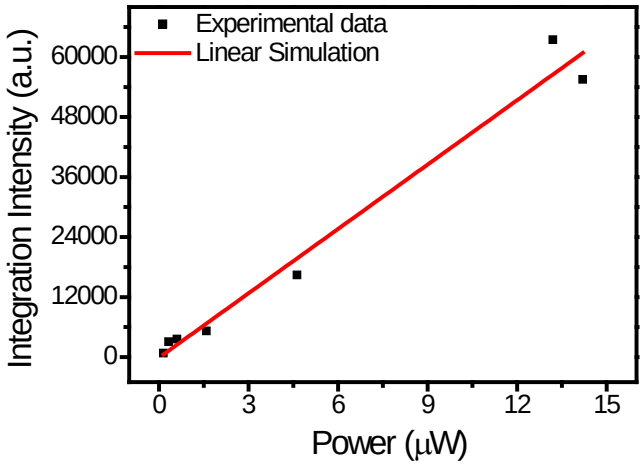

Fig. S3 Integration intensity recorded by the spectrometer as a function of the power of input light, the exposure time is 50 ms.

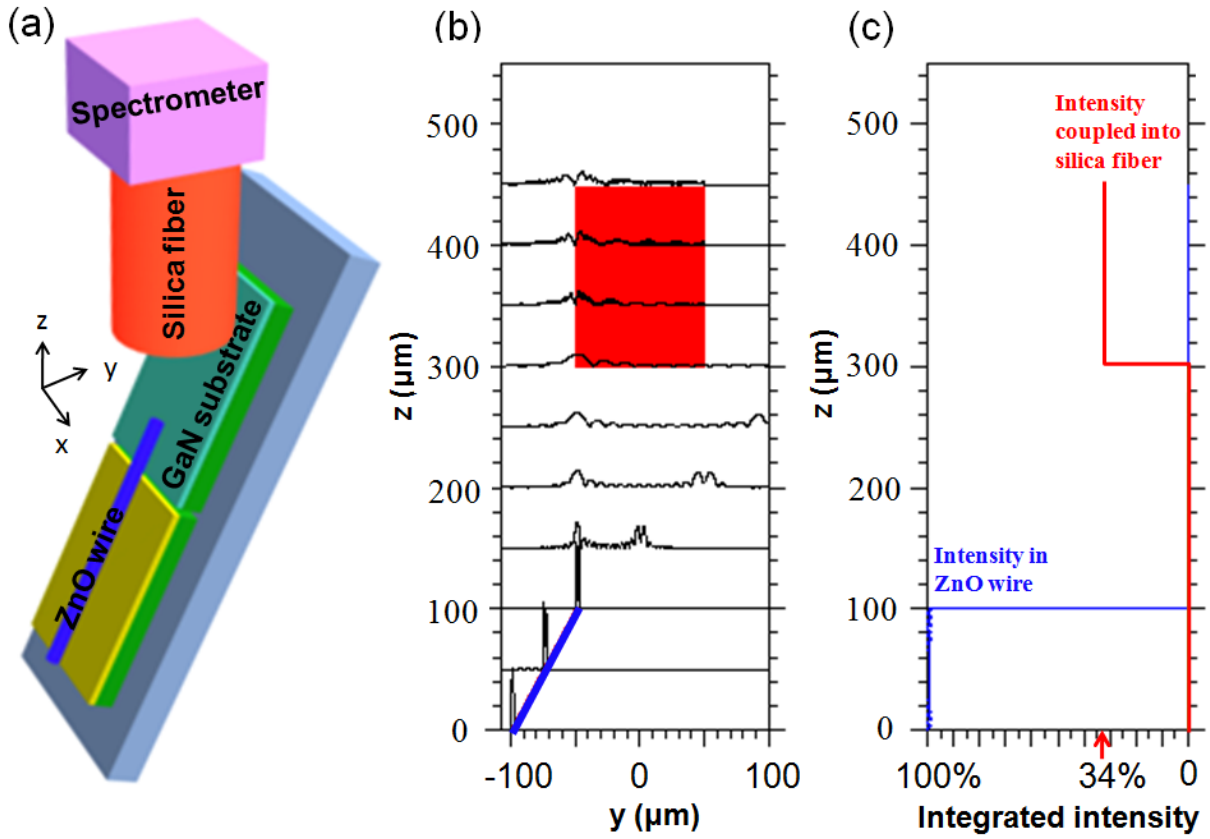

Fig. S4 Method to measure the external efficiency of a single wire LED. A multimode silica optical fiber connected to the spectrometer was used to detect the light from the single NW LED. The emission power of the LED is calculated using the linear relationship in Fig. S3 considering the coupling efficiency of 34% from the LED to optical fiber. (a) Schematic diagram to measure the output power of the single wire LED. (b) Simulated results on the light profile slices in ZnO wire and silica fiber over the y-z planes. (c) Stimulated coupling efficiency of the light from ZnO wire to silica fiber. The blue curve represents the emission power in ZnO wire while the red curve represents the power coupling from the ZnO wire into the optical fiber. The diameters of the ZnO wire and silica fiber are 3 μm and 100 μm, respectively. The refractive indexes of ZnO and silica fiber are 2.08 and 1.45, respectively. The angle between them is about 30°. We simulated the propagation and coupling behavior by using a software program (BPM RSOFT) based on the beam-propagation method. The coupling efficiency of the structure we used in the experiment is about 34%.

B. Characterization of the as-fabricated LED before applying strain

Before the electromechanical and optical measurements, we first measured the original optoelectronic performance of the device without strain. The current-voltage (I-V) characteristic of a single n-ZnO wire/p-GaN substrate LED device is shown in Fig. S5a. The I-V curve clearly shows a nonlinear increase of current under the forward bias, which indicates reasonable p–n junction characteristics and the possibility of light emission. The turn-on voltage of the hybrid heterojunction of ZnO/GaN (wire/film) is around 3 V. The emission spectrum of the as-fabricated LED was monitored at different biased voltages/injection-currents at room temperature. Peak-deconvolution of the emission spectra using Gaussian functions (inset picture in Fig. S5b) shows that the blue/near-UV emission spectrum consists of a distinct peak centered at 390-395 nm and a long red tail until 460 nm. In order to analysis the peak position shift under biased voltage and strain, we use two emission bands centered at 405-415 nm and 420-440 nm in the deconvolution to represent the long red tail in blue/near-UV emission spectrum considering two interface states at GaN side and ZnO side of the heterojunction, respectively.

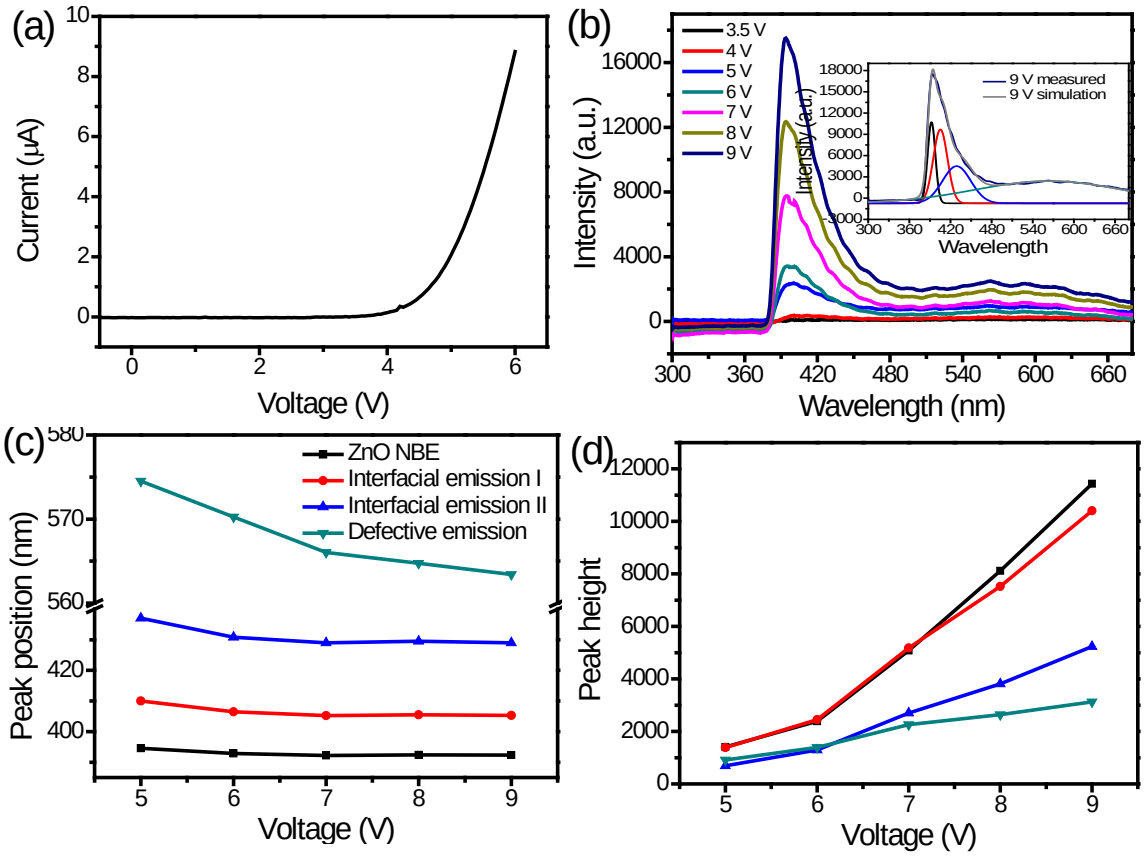

Fig. S5. Characteristics of a single wire LED without applying strain. (a) I-V characteristics of the LED. (b) EL spectrum as a function of the forward biased voltage. Inset image shows the Gaussian deconvolution analysis of the EL emission (c) Four emission bands peak position as a function of the biased voltage. (d) Peak height as a function of the biased voltage.

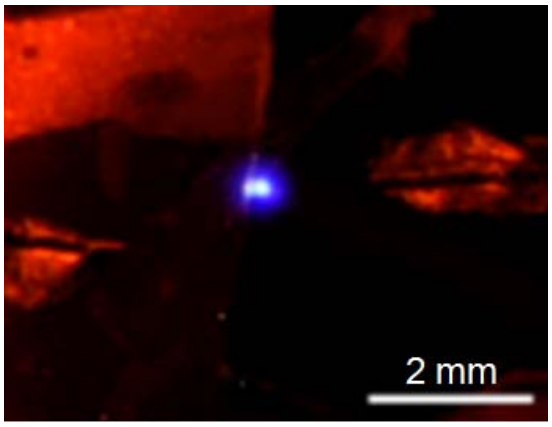

Fig. S6 Digital camera images of a single n-ZnO nanowire/p-GaN LED with weak background light illumination. The blue light spot at the middle is the light from a 3 μm-diameter single ZnO wire LED.

C. Evidence supporting the model presented

With considering the non-ideal flatness of the GaN substrate and the possible loose contact between ZnO wire and the substrate, one my worry about the instability at the p-n interface area during mechanical straining. We have done a set of experiments to prove that this is not the case, and the model presented in Fig. 3 is the most likely explanation to the observed phenomenon, as listed in follows.

C1. Stability of the device over a period of time

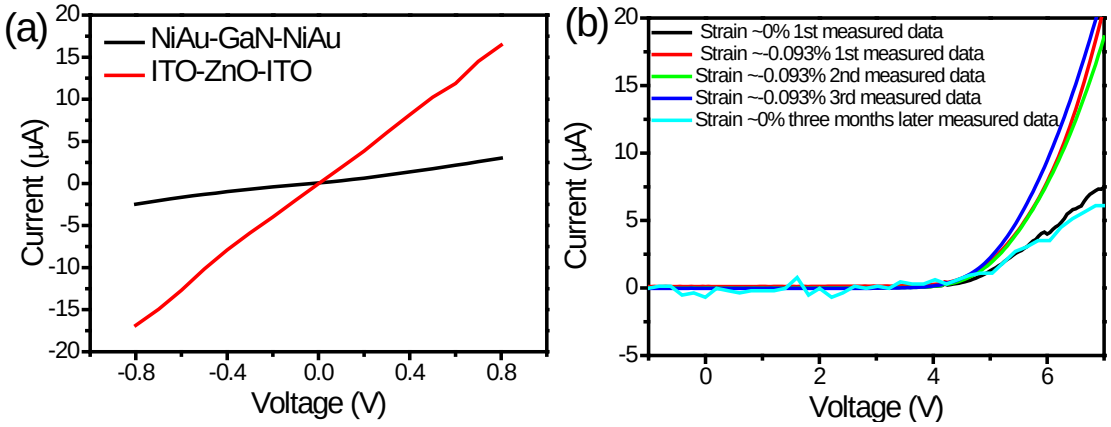

Fig. S7 (a) I-V curves of Ni/Au-GaN-Ni/Au contacts and ITO-ZnO-ITO contacts. The nearly Ohmic contacts and large current at small bias voltage (0.8V) confirms that the rectifying I-V curves of our devices come from the p-n diode. (b) I-V curve of a single wire LED under the same strain measured at different time and I-V curve of the device after keeping it in dry cabinet for three months, showing its great stability.

C2. Effect of polar directions

ZnO has a polar direction that is along its c-axis, which is the growth direction of the wires. During the fabrication of the devices, there is a 50% chance for the wires to be oriented with c-axis pointing from ITO side to the GaN side, while the other 50% are oriented in reverse direction. In the main text, we have presented the data for the former case (see Figs. 1-3). Here present the latter case in Fig. S8.

The data shown in Fig. S8 indicate that the improved contact between the wire and the GaN substrate may not be responsible to the change of emission intensity, rather it is likely due to the piezoelectric effect as described in the text.

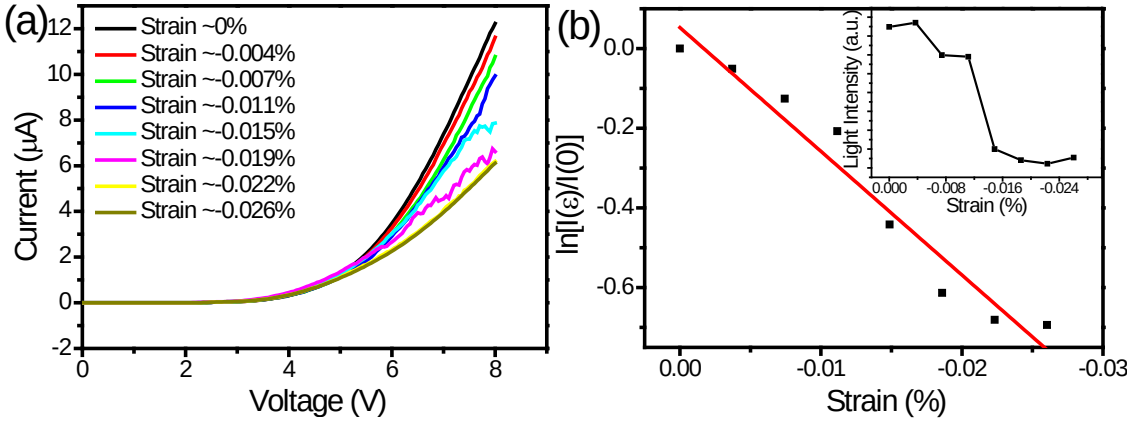

Fig. S8 Electronic and optical characteristics of a ZnO wire LED whose injection current and emission light intensity decreases with the increase of a-axis compressive strain. (a) I-V curve of the LED under different strain. (b) Plot of ln[I(ε)/I(0)] at 8 V biased voltage under different strain, the inset shows the change of light intensity at 8 V biased voltage under different strain. Such result is possible if the c-axis of the wire is oriented pointing away of the GaN side (see main text).

C3. Linear relationship between the logarithm of the injection current and the applied strain

From the theory presented in Section F, a linear relationship is expected between the logarithm of the injection current and the applied strain. This is consistent to the data presented in Fig. 1d and Fig. S8. This is another evidence proving that a possible change in contact area between n- and p-side of the device was not responsible to the observed increase in efficiency.

D. Band diagram of (n-ZnO wire)-(p-GaN film) heterojunction and analysis of the EL spectra

Band-line-up data for the ZnO/GaN heterostructure are needed for analyzing the emission characteristics of the LED. ZnO and GaN have a type-II band offset. The ideal heterojunction band diagram for n-ZnO/p-GaN is constructed by following the Anderson model[1]. To construct the diagram, the band gap energies of ZnO and GaN are assumed to be 3.3[2-4] and 3.4 eV[3-5], respectively. The electron affinities of ZnO and GaN are assumed to be 4.5 eV[6, 7] and 4.1 eV[8, 9]. The valence band offset here is about 0.3 eV, which is in the range of valance band offset values reported for ZnO/GaN heterojunction from 0.13 eV to 1.6 eV[3-5, 10-13]. The origin of light emission could be analyzed based on the schematic band diagram and through comparison of photoluminescence (PL) and EL spectra (Fig. S9). Two UV peaks in the PL spectra of ZnO wire centered at 376 nm (3.30 eV) and 391 nm (3.17 eV), correspond to the bandgap recombination and phonon assisted exciton emission, respectively[2, 3]. Three UV peaks in the PL spectra of GaN film centered at 362 nm (3.40 eV), 377 nm (3.29 eV) and 390 nm (3.18 eV) correspond to the bandgap recombinations and Mg acceptor related emission[3, 5] (acceptor activation energy for Mg in GaN is about 0.14-0.21 eV), respectively.

There has been a controversy about the emission origination in ZnO/GaN heterojunction LED[4, 5, 10,

[14]. It is shown in Fig. S9b the EL emission overlaps with 390 nm peak in ZnO PL and has a long red tail until 460 nm. Peak-deconvolution of the EL spectra using Gaussian functions (inset picture in Fig. S5b) shows that the spectrum consists of a distinct peak centered at 390-395 nm, a long red tail until 460 nm and a weak yellow emission at around 570 nm. According to the PL spectra, the band centered in the range of 390-395 nm could be attributed to the phonon assisted excitonic emission in ZnO wire. Shorter wavelength emission from GaN film and ZnO wire may be reabsorbed by ZnO wire, therefore, there is no peak shorter than 390 nm. However, the tail emission (ranged from UV peak to 460 nm) has no corresponding band in individual PL spectra of ZnO or GaN. Referring to the band diagram, the tail emission may be attributed to interfacial emission that comes from the radiative interfacial recombination of the electrons from n-ZnO and holes from p-GaN[5, 10, 15, 16]. There is a discontinuity at the interface, and this abrupt discontinuity may influence the EL spectra. The energy of the electrons and holes at this discontinuity interface is not a fixed value as shown in Fig. S9a, but has a range of variation. Therefore, the interfacial emission should be a red broad tail emission in UV range[10]. The interface states are like incorporating of one compound into the other in some respects. The incorporation of one compound into the other would lead to a reduced bandgap as compared to that of either ZnO or GaN. Density functional theory calculation reveals that incorporation GaN cluster in a ZnO host results in a more effective bandgap reduction than incorporating ZnO in a GaN host[17]. In order to analysis the peak position shift under biased voltage and strain, we use two emission bands centered at 405-415 nm and 420-440 nm in the deconvolution to represent the long red tail in blue/near-UV emission spectrum considering two interface states at GaN side and ZnO side of the heterojunction, respectively.

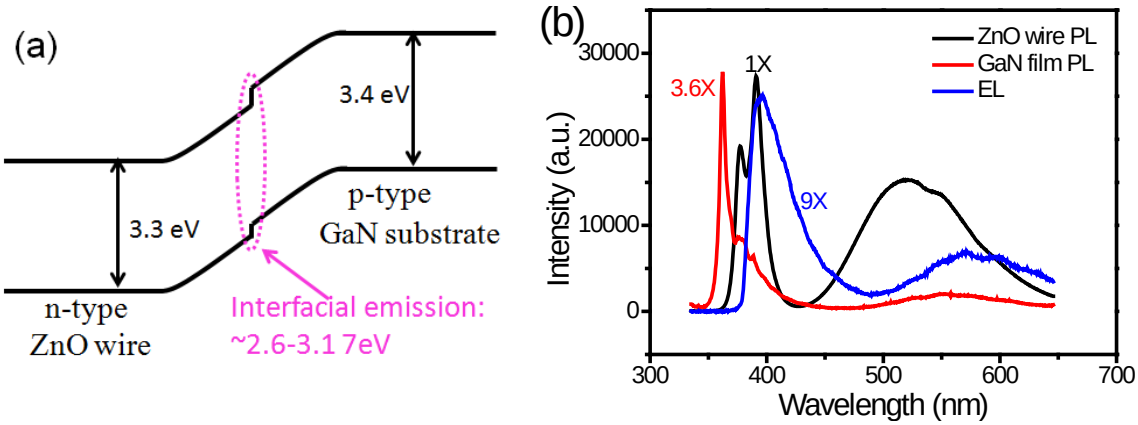

Fig. S9. (a) Schematic energy band diagram of a p-n junction without strain. (b) Photoluminescence and spectra of a single ZnO wire and GaN film and electroluminescence spectrum of a single wire LED.

E. Effect of strain on band profile of (n-ZnO wire)-(p-GaN film) heterojunction

In LED, the output photon intensity in an unstrained and a strained LED could be given by[18]:

$$\Phi_{out}(0) = \eta_{ex}(0)\frac{I(0)}{e} = mh\nu\eta_e(0)\eta_i(0)\frac{I(0)}{e} \qquad (S1)$$

$$\Phi_{out}(\varepsilon) = \eta_{ex}(\varepsilon)\frac{I(\varepsilon)}{e} = mh\nu\eta_e(\varepsilon)\eta_i(\varepsilon)\frac{I(\varepsilon)}{e} \quad \text{(S2)}$$

where m represents the percentage of the light being probed by the spectrometer or CCD, Φ_{out} is the recorded output light intensity, η_{ex} is the external efficiency, which describes the ratio of externally produced photon flux to the inject electron flux; η_e is the overall extraction efficiency that is related to the absorption and reflection of the light in the device; η_i is therefore simply the ratio of the generated photon flux to the electron injection flux. Strain will affect the output light intensity of LED through the effect on external efficiency and the amount of injection current.

A negative piezopotential along c-axis will be induced in the wire under in-plane a-axis compressive strain (Fig. 3b). The local band structure and internal field near the p-n junction will be changed/modified (Fig. 3a) including barrier height modification and band bending. In order to simplify the problem, we investigate the barrier height modification and band bending effects separately.

For barrier height modification, according to the Schokley equation, the p-n junction I-V characteristics without strain can be described as[19]:

$$I(0) = I_0(e^{qV_A/nkT} - 1) \sim I_0 e^{qV_A/kT} \quad \text{if } V_A \gg kT/q \quad \text{(S3)}$$

$$I_0 = qA\left(\frac{D_N}{L_N}\frac{n_i^2}{N_A} + \frac{D_P}{L_P}\frac{n_i^2}{N_D}\right) \quad \text{(S4)}$$

where q the unit electron charge, V_A is the external voltage on the p-n junction, T the temperature, n_i intrinsic carrier density. D_N, L_N, and N_A are referred to as diffusion coefficient and diffusion length of minority carrier holes, total number of acceptor density in a p-type material, respectively. D_P, L_P and N_D are referred to as diffusion coefficient and diffusion length of the minority carrier electrons, total number of donor density in an n-type material, respectively. Assuming that the piezopotential drop across the junction is $\Delta\Psi$, the current flow through the p-n junction under strain can be described as:

$$I(\varepsilon) = I_0(e^{(qV_A+\Delta\Psi)/kT} - 1) \sim I_0 e^{\frac{qV_A+\Delta\Psi}{kT}} \quad \text{if } (V_A + \Delta\Psi) \gg kT/q \quad \text{(S5)}$$

The change of current with strain can be determined by[20]:

$$ln\left(\frac{I(\varepsilon)}{I(0)}\right) = \Delta\Psi/kT \quad \text{(S6)}$$

When an in-plane stress σ_{xx} is added on the wire, the y-direction and z direction of the NW is free. The finite-element analysis method (COMSOL) is used to calculate the stress and piezopotential in the wire[21].Generally speaking, according to the conventional theory of piezoelectricity and elasticity, the mechanical equilibrium and the direct piezoelectric effect can be described by the coupled constitutive equation:

$$\begin{cases} \sigma_p = c_{pq}\varepsilon_q - e_{kp}E_k \\ D_i = e_{iq}\varepsilon_q + \kappa_{ik}E_k \end{cases} \quad \text{(S7)}$$

where σ is the stress tensor, ε is the strain, E is the electric field, and D is the electric displacement. κ_{ik} is the dielectric constant, e_{iq} is the piezoelectric constant, and c_{pq} is the mechanical stiffness tensor. By

considering the C_{6v} symmetry of a ZnO crystal (with wurtzite structure), c_{pq}, e_{kp}, and κ_{ik} can be written as:

$$c_{pq} = \begin{vmatrix} c_{11} & c_{12} & c_{13} & 0 & 0 & 0 \\ c_{12} & c_{11} & c_{13} & 0 & 0 & 0 \\ c_{13} & c_{13} & c_{33} & 0 & 0 & 0 \\ 0 & 0 & 0 & c_{44} & 0 & 0 \\ 0 & 0 & 0 & 0 & c_{44} & 0 \\ 0 & 0 & 0 & 0 & 0 & \frac{(c_{11}-c_{12})}{2} \end{vmatrix} \quad \text{(S7.1)}$$

$$e_{kp} = \begin{vmatrix} 0 & 0 & 0 & 0 & e_{15} & 0 \\ 0 & 0 & 0 & e_{15} & 0 & 0 \\ e_{31} & e_{31} & e_{33} & 0 & 0 & 0 \end{vmatrix} \quad \text{(S7.2)}$$

$$\kappa_{ik} = \begin{vmatrix} \kappa_{11} & 0 & 0 \\ 0 & \kappa_{11} & 0 \\ 0 & 0 & \kappa_{33} \end{vmatrix} \quad \text{(S7.3)}$$

For ZnO, we have c_{11} = 207 GPa, c_{12} = 117.7 GPa, c_{13} = 106.1 GPa, c_{33} = 209.5 GPa, c_{44} = 44.8 GPa, and c_{55} = 44.6 GPa. The relative dielectric constants are κ_{11} = 7.77 and κ_{33} = 8.91, and the piezoelectric constants are e_{31} = -0.51C/m^2, e_{33} = 1.22C/m^2, and e_{15} = -0.45C/m^2 [21].

The electrostatic behavior of charges can be described by Poisson equation:

$$\nabla \cdot D = \rho(x, y, z) \quad \text{(S8)}$$

where D is the electric displacement, ρ is the charge density. For a one-dimensional problem, this reduces to a more useful form of:

$$\kappa_{ik} \frac{d^2 \Delta\psi_i}{dx^2} = -\kappa_{ik} \frac{d\Delta E}{dx} = -\rho \quad \text{(S8.1)}$$

where ψ_i is electrical potential. The conductivity of the ZnO is ignored in the simulation for simplicity, which is valid if the density of doping/vacancy is low, which means:

$$\nabla \cdot D = \rho(x, y, z) = 0 \quad \text{(S8.2)}$$

In order to solve the problem, we also need the mechanical equilibrium condition assuming there is no body force on the wire:

$$\nabla \cdot \sigma = 0 \quad \text{(S9)}$$

The compatibility equation is a geometrical constraint that must be satisfied by strain ε:

$$e_{ilm}\, e_{jpq} \frac{\partial^2 \varepsilon_{mp}}{\partial x_l\, \partial x_q} = 0 \quad \text{(S10)}$$

The fully coupled equations S7-S10 along with appropriate boundary conditions give a complete description of a static piezoelectric system. Figure 3b shows the stress and piezopotential distribution in a ZnO wire under compressive strain calculated by finite element method using the software COMSOL.

The maximum potential along the c-axis can also be estimated assuming there is a uniform stress along a-axis of the wire ($\sigma_{xx} \neq 0$, other σ=0) and only considering the direct piezoelectric effect:

$$|\Delta\Psi| \sim (e_{31}\varepsilon_{xx} + e_{31}\varepsilon_{yy} + e_{33}\varepsilon_{zz}) L_\varepsilon / \kappa \quad \text{(S11)}$$

where e_{31}, and e_{33} are the linear piezoelectric coefficients, ε_{xx}, ε_{yy} and ε_{zz} strain tensor along a, b and c axis of the wire, L_ε the effective length of the wire under strain. Equation S11 shows that piezopotential has a

linear relationship with the external strain. Generally, combining equations S5, S6 and S11, we can expect that $ln\left(\frac{I(\varepsilon)}{I(0)}\right)$ of the p-n junction have a linear relationship with the external strain (Fig. 1d).

The localized positive piezopotential of ZnO near the interface will induce band bending to form electron and hole channels (Fig. 3a) near the ZnO/GaN interface which can be predicted from Poisson equation[19]. The piezopotential is solved by the Poisson equation by assuming that the piezoelectric charge distribute near the interface of a p-n junction within a width of W_{piezo} as shown in Fig. 3a:

$$\kappa_{ik}\frac{d^2\Delta\psi_i}{dx^2} = -\Delta\rho(x) = -\rho_{piezo}(x) \qquad \text{(S12)}$$

We got the solution when assuming ρ=0 outside the piezo-charge area as the boundary conditions:

$$\Delta\psi(x) = \frac{1}{\kappa}\rho_{piezo}\left(W_{piezo} - \frac{x}{2}\right)x \qquad \text{for } 0 \le x \le W_p \qquad \text{(S12.1)}$$

$$\Delta\psi(x) = \frac{1}{2\kappa}\rho_{piezo}W_{piezo}^2 \qquad \text{for } x > W_p \qquad \text{(S12.2)}$$

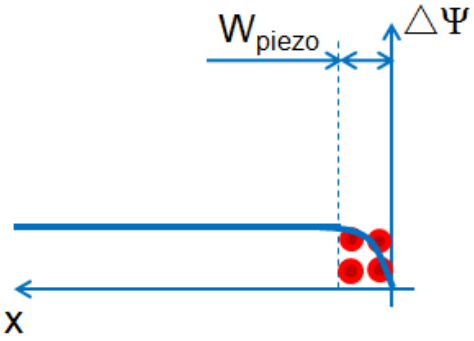

Fig. S10. Potential profile along the x-axis (the –c axis of ZnO wire) assuming positive piezo-charges (red dots) distribute within a width of W_{piezo} adjacent to the interface.

The potential profile is depicted in Fig. S10. The band profile under strain is the coupling of piezopoential and strain free band profile of p-n junction (the red line in the lower image of Fig. 3a). Thus, a negative drop will form near the interface. If the drop is large enough in a small distance, electron and hole channels will be created near the interface. Electrons and holes are to be trapped in the electron and hole channels, respectively. The trapped holes increase the holes injection from p-GaN to n-ZnO, which will increase the recombination efficiency between electrons and holes near the interface. Combining equations S1, S2 and equation S6, the output light intensity of the LED under strain is related to the injection current and external efficiency under strain by:

$$\ln\left(\frac{\Phi_{out}(\varepsilon)}{\Phi_{out}(0)}\right) = ln\left(\frac{I(\varepsilon)}{I(0)}\right) + ln\frac{\eta_{ex}(\varepsilon)}{\eta_{ex}(0)} = \frac{\Delta\Psi}{kT} + f(\varepsilon) \qquad \text{(S13)}$$

where f(ε) represents the dependence of the external efficiency including extraction efficiency and internal efficiency on strain. If the recombination efficiency can be increased by strain, it is expected that the rate at which the light output increases is larger than that the current increases. It is pointed out that though the band offset values varies in different reports[3-5, 10-13], and is dependent on the fabrication

process of the heterojunction, the band offset value doesn't affect the band shift and bending induced by piezopotential.

F. The effect of strain on light propagation in ZnO wire

The photoelastic effect can be investigated by studying the light polarization under different strain. Electroluminescence light propagates along the wire and oscillates in the wire due to interfere as a result of the end surface reflection. The transmittance obeys the Airy equation[22]:

$$\Phi_T = \Phi_0 \frac{1}{1+F\sin^2(\theta/2)} \quad \text{(S14)}$$

$$\theta = 2\pi s/\lambda \quad \text{(S15)}$$

$$F = 4R/(1-R)^2 \quad \text{(S16)}$$

$$s = 2nL \quad \text{(S17)}$$

where Φ_T is the intensity of the transmitting light detected by CCD camera, and Φ_0 is the total propagating light intensity including the reflecting and transmitting light, R is reflectivity, n is the refractive index, L is the length of the wire, s is the optical path, λ is the light wavelength.

It is known that the refractive index n of ZnO is changed under strain, which will change the optical path and the phase of the transmitting light reaching the end of the wire[18].

$$s = s_0 + \Delta s = 2n_0L + 2\Delta nL_\varepsilon = 2n_0L + 2 \times \frac{1}{2} n^3 \beta \sigma L_\varepsilon \quad \text{(S18)}$$

$$\sigma = E\varepsilon \quad \text{(S19)}$$

where n_0 is the native refractive index without strain, L is the total length of the wire, L_ε is the effective length of the wire under strain, β is the photoelastic coefficient, σ is the applied stress on the wire, ε is the applied strain on the wire, E is the Young's modulus of ZnO. LED is a result of spontaneous emissions polarized at various angles, but the guiding mode propagating along the ZnO wire is dominated by the $P_\perp$ modes whose polarization direction is perpendicular to the wire. Therefore, Airy equation for the $P_\perp$ mode light of ZnO wire under strain could be written as:

$$\Phi_{out}^{\perp} \sim \Phi_0^{\perp} \frac{1}{1+F\sin^2[(2\pi n_0 L + \pi n_0^3 \beta E\, \varepsilon L_\varepsilon)/\lambda]} \quad \text{(S20)}$$

where $\Phi_T^{\perp}$ is the transmitting light intensity in the $P_\perp$ modes detected by CCD camera, and $\Phi_0^{\perp}$ is the total propagating light intensity that including the reflecting and transmitting light. Since the large aspect ratio of the wire, the effect of strain on the optical path of the $P_\parallel$ modes is much smaller than that on $P_\perp$ modes, The ratio of $\Phi_{out}^{//} / \Phi_{out}^{\perp}$ can be described by the equation[22]:

$$\Phi_{out}^{//} / \Phi_{out}^{\perp}(\varepsilon) \sim \{1 + \frac{4R}{(1-R)^2} \sin^2[\frac{\pi 2\pi n_0 L + \pi n_0^3 \beta E\, \varepsilon L_\varepsilon}{\lambda}]\} \quad \text{(S21)}$$

According to the equation, when the change of optical path equals one wavelength λ,

$$\delta s = n^3 \beta E(\delta\varepsilon) L_\varepsilon = \lambda \quad \text{(S22)}$$

the phase will have a change of 2π, corresponding to a period of $\Phi_{out}^{//}/\Phi_{out}^{\perp}$ modulation by changing strain (see Fig. 4b). Thus,

$$\delta\varepsilon = \frac{\lambda}{n^3\beta E}\frac{1}{L_\varepsilon} = b\frac{1}{L_\varepsilon} \quad \text{(S23)}$$

where b the slope of the line curve in Fig. 4d. The photoelastic coefficient could be derived by:

$$\beta = \frac{\lambda}{bn^3E} \quad \text{(S24)}$$

Fig. 4d shows the strain periods δε versus the inverse of the length of the wire under strain ($1/L_\varepsilon$). The strain period δε can be derived from the data simulation (Fig. 4b). Four periodes of strain δε are 0.031%, 0.040%, 0.057% and 0.062%, and the measured effective length are 368.0, 335.1, 220.6 and 194.4 μm, respectively. The Young's modulus of ZnO and polystyrene are about 129 GPa and 3 GPa, respectively. It can be seen that there is a linear relationship between δε and $1/L_\varepsilon$. From the slope of the curve, we can calculate the photoelastic coefficients which is 3.20×10^{-12} m^2/N (395 nm wavelength). The piezooptic coefficient value is consistent to the reported value for ZnO[23, 24].

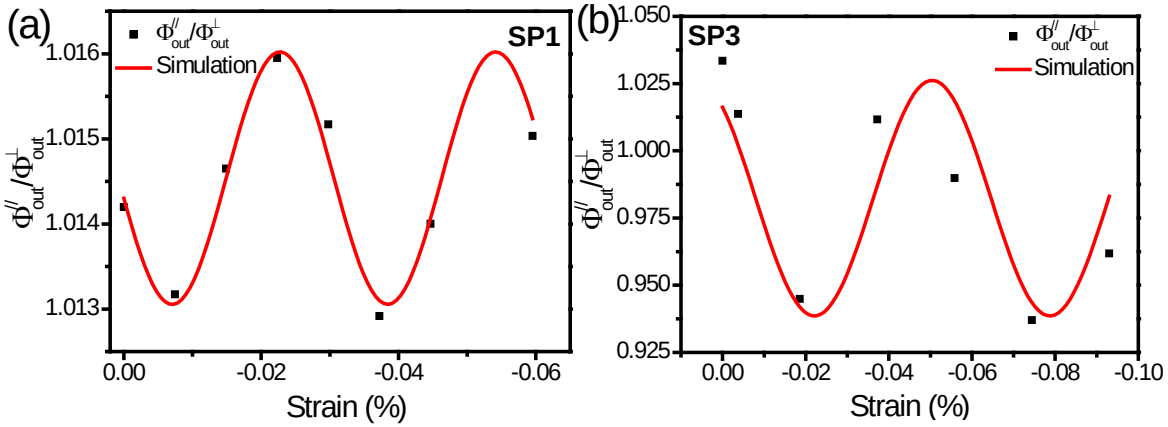

Fig. S11. $\Phi_{out}^{//}/\Phi_{out}^{\perp}$ as a function of strain of devices for devices SP1 and SP3, which are plotted in Fig. 4d.

References

1. Anderson, R. L. *Solid State electron.* **1962**, *5*, 341.
2. Özgür, Ü.;Alivov, Y. I.; Liu, C.; Teke, A.; Reshchikov, M. A.; Dogan, S.; Avrutin, V.; Cho, S. J.; Morkoc, H. *J. Appl. Phys.* **2005**, *98*, 041301.
3. Liu, H. F.; Hu, G. X.; Gong, H.; Zang, K. Y.; Chua, S. J. *J. Vac. Sci. Technol. A* **2008**, *26*, 1462.
4. Alivov, Y. I.; Van Nostrand, J. E.; Look, D. C.; Chukichev, M. V.; Ataev, B. M. *Appl. Phys. Lett.* **2003**, *83*, 2943.
5. Xu, S.; Xu, C.; Liu, Y.; Hu, Y. F.; Yang, R. S.; Yang, Q.; Ryou, J. H.; Kim, H. J.; Lochner, Z.; Choi, S.; Dupuis, R.; Wang, Z. L. *Adv. Mater.* **2010**, *22*, 4749.

6. Wang, Z. L.; Song, J. H. *Science* **2006**, *312*, 242.
7. Sundaram, K. B.; Khan, A., *J. Vac. Sci. Technol. A* **1997**, *15*, 428.
8. Bougrov, V.; Levinshtein, M. E.; Rumyantsev, S. L.; Zubrilov, A. *Properties of Advanced SemiconductorMaterials GaN, AlN, InN, BN, SiC, SiGe*; Wiley-Interscience: New York, 2001.
9. Titkov, I. E.; Zubrilov, A. S.; Delimova, L. A.; Mashovets, D. V.; Liniichuk, I. A.; Grekhov, I. V. *Semiconductors* **2007**, *41*, 564.
10. Hwang, D.K.; Kang, S. H.; Lim, J. H.; Yang, E. J.; Oh, J. Y.; Yang, J. H.; Parka, S. J. *Appl. Phys. Lett.* **2005**, *86*, 222101.
11. Nakayama, T.; Murayama,M. *J. Cryst. Growth* **2000**, *214/215*, 299.
12. Johnson, M. A. L.; Fujita, S.; Rowland, W. H.; Hughes, W. C.; Cook, J. W.; Schetzina, J. F. *J. Electron. Mater.* **1996**, *25*, 855-862.
13. Hong, S. K.; Hanada, T.; Makino, H.; Chen, Y. F.; Ko, H. J.; Yao, T.; Tanaka, A.; Sasaki, H.; Sato, S. *Appl. Phys. Lett.* **2001**, *78*, 3349.
14. Cole, J. J.; Wang, X.; Knuesel, R. J.; Jacobs, H. O. *Nano Lett.* **2008**, *8*, 1477.
15. Reshchikov, M. A.; Morkoc, H. *J. Appl. Phys.* **2005**, *97*, 061301.
16. Alivov, Y. I.; Ozgur, U.; Dogan, S.; Liu, C.; Moon, Y.; Gu, X.; Avrutin, V.; Fu, Y.; Morkoc, H. *Solid State Electron.* **2005**, *49*, 1693.
17. Huda, M. N.; Yan, Y.; Wei, S. H.; Jassim, M. M. A. *Phys. Rev. B* **2008**, *78*, 195204.
18. Saleh, B. E. A.; Teich, M. C. *Fundamentals of Photonics*; Wiley-Interscience: New York, 1991.
19. Sze, S. M. *Physics of Semiconductor Devices*; Wiley-Interscience: New York, 1981.
20. Zhou, J.; Gu, Y. D.; Fei, P.; Mai, W. J.; Gao, Y. F.; Yang, R. S.; Bao, G.; Wang, Z. L. *Nano Lett.* **2008**, *8*, 3035.
21. Gao, Y. F.; Wang, Z. L. *Nano Lett.* **2007**, **7**, 2499.
22. Born, M.; Wolf, E. *Principles of Optics*; Pergamon Press: Oxford, 1980.
23. Ebothe, J.; Gruhn, W.; Elhichou, A.; Kityk, I. V.; Dounia, R.; Addou, A. *Opt. Laser Technol.* **2004**, *36*, 173.
24. Vedam, K.; Davis, T. A. *Phys. Rev.* **1969**, *181*, 1196.